Proceedings of the 28th IEEE
EMBS Annual International Conference
New York City, USA, Aug 30-Sept 3, 2006

A Novel Active Contour Model Using Local and Global Statistics for Vessel Extraction

K. W. Sum and Paul Y. S. Cheung, *Senior Member, IEEE*

***Abstract*— Vessel extraction is one of the critical tasks in clinical practice. Most of the deformable models used in these applications are based on either image gradient or global statistics of the intensity as their curve evolution and stopping criteria. However, the models using global statistic alone are not adaptive to the uneven intensity distribution since they do not take local variations in the area of interest into consideration. In this paper, we propose a novel level set based active contour model which combines a simple local function with the global statistical information for better vessel extraction results.**

***Index Terms*— Active contours, level set method, narrow-band, vessel extraction, medical image analysis.**

I. INTRODUCTION

Active contours, snakes [1][2][3], or deformable models have been widely used in many applications, including edge detection, shape modeling, motion tracking, and image segmentation. Level set based active contours can handle complex object boundaries by flexible curve evolutions. In addition, since the level set function is defined in the Euclidean space, it is easily extendable to higher dimensions. The level set method is first introduced for front propagation by Osher and Sethian in [4]. It is then applied in shape recovery and isolation of shape from its background by Malladi and Sethian in [5]. This concept provides a good alternative to the classical deformable models and has been widely used in medical image analysis. There are a number of active contour models developed based on level set methods. They include the geometric active contour model [6] based on the mean curvature motion and the geodesic active contour model [7] which defines the problem in a Riemannian space.

Most of these snake and active contour models make use of local image gradient. This local image property may possibly lead the curve evolution to stop at local minima. In the case that the object is not precisely defined by its edges, the model may not correctly find the object. Chan and Vese [8] developed another active contour model using region-based statistics. Instead of using local image gradient, this model measures the global statistical properties of the object to adjust the level set function and fit the object with the zero level set. Consequently, the resultant detected object is not necessarily defined by its edges.

K. W. Sum is with Department of Electrical and Electronic Engineering, University of Hong Kong, Pokfulam, Hong Kong (e-mail: kwsum@eee.hku.hk)

Paul Y. S. Cheung is with the Department of Electrical and Electronic Engineering, University of Hong Kong, Pokfulam, Hong Kong (e-mail: cheung@eee.hku.hk)

However, in most natural or medical images, the objects are not homogenous in intensity. In addition, the intensity distribution of the image is normally not even. The uneven intensity distributions may be due to the limited exposure to minimize side effects to the patient in X-ray images, the projection of 3D object to 2D image through different depths, or artifacts of different imaging techniques.

In this paper, we propose a model which combines both global and local image properties to achieve more accurate object extraction. This is found to greatly improve the curve evolution for medical image object detection.

The model will be demonstrated with some clinical angiograms. The complex nature of angiograms provides many challenging problems which are typical of many medical images. The vessel structure is physically complex in three dimensions and vessel extraction is one of the critical tasks in medical imaging [9]. After different imaging methods, the vasculature may not be clearly shown in the 2-D image when projected from the original 3-D depth structure. In this case, the traditional active contours cannot extract the vessel correctly.

This paper is organized as follows: In Section II, the concept and formulation of our model is described in details. In Section III, the numerical implementation of our model is presented. In Section IV, our model is applied on angiograms in contrast with Chan-Vese model. Finally, the conclusions are given in Section V.

II. DESCRIPTIONS OF THE MODEL

Our model is defined based on techniques of curve evolution, statistical function, and level set methods. Traditional level set method uses either the image gradient or the global statistics as evolving term [5][8].Either one of them is not adequate for the complexity in medical image analysis. In our model, we combine both global and local image properties to overcome the uneven intensity distribution in the image and provide better object extraction.

We define the target object as an open subset ω of Ω (i.e. $\omega \subset \Omega$) where Ω is the entire image space. The evolving curve C in Ω is defined as the boundary of the open subset ω (i.e. $C = \partial\omega$). Therefore, the area inside C denotes the region ω which is the object body, and the area outside C denotes the region $\Omega\backslash\omega$ which is the background. The overall energy function $J(C)$ consists of one global term $F_G(C)$ and one local term $F_L(C)$,

$$J(C) = \alpha\, F_G(C) + \beta\, F_L(C) \tag{1}$$

where α and β is the regulating parameters between the global and local terms.

A. Global Term

The global term is defined based on the global properties, such as the image statistics and measures of the curve C. We define the global term based on the formulation in [8]. Let Ω be a bounded open subset of $\mathbf{R}^2$.

$$\begin{aligned} F_G(C) &= \mu\, Length(C) + \\ &\quad \lambda_1 \int_{\omega} |u_o(x,y) - c_1|^2 dxdy + \\ &\quad \lambda_2 \int_{\Omega\setminus\omega} |u_o(x,y) - c_2|^2 dxdy \end{aligned} \tag{2}$$

where μ, λ_1, and λ_2 are the regulating parameters; $Length(C)$ is defined as the length of the curve C; u_o is the image intensity; c_1 and c_2 are the average intensity inside and outside C respectively.

B. Local Term

We introduce the local term as the key to improve the existing models, which use global statistics alone, for better vessel extraction capability. It will be combined with the global term in the level set formulation. Before we define the local term, let us define the concept of narrow band since the local term in our model will only be applied in the narrow band. The concept and definition of narrow band is adopted from [5]. However, in our method, the narrow band technique is not only used to reduce the computation time, which is the case in [5], but also confine the object area and avoid noisy segmentation whenever the local term is applied.

The narrow band Φ is the region bounded on either side of the zero level set by two curves which are at a distance $\delta/2$ from the zero level set. Throughout the curve evolution process, the level set function ϕ is re-initialized and the narrow band is also re-calculated and updated for every evolution. The area inside C and within the narrow band denotes the region σ, and the area outside C and within the narrow band denotes the region $\Phi\setminus\sigma$.

Now, we define the local term as follows:

$$\begin{aligned} F_L(C) &= \lambda_3 \int_{\sigma} |u_N(x,y) - m_1|^2 dxdy + \\ &\quad \lambda_4 \int_{\Phi\setminus\sigma} |u_N(x,y) - m_2|^2 dxdy \end{aligned} \tag{3}$$

where λ_3 and λ_4 are the regulating parameters, u_N is the local contrast image defined as in (4), m_1 and m_2 are the average values of u_N inside and outside C respectively.

$$u_N(x,y) = \frac{u_o(x,y) - M_1}{M_2 - M_1} \times M_g \tag{4}$$

The local contrast image u_N is generated by a sliding-neighborhood operation with a $N \times N$ spatial neighborhood window. This operation adaptively and locally increases the range of the image intensity from u_o to u_N. M_1 and M_2 are the minima and maxima of u_o among the elements of the neighborhood window. M_g is the maximum grey level value of the original image. At a result, the local contrast image u_N emphasizes the local intensity variations of the original image and fits into the local term formulation.

In the local term, the elements of the local contrast image is compared with the average values of the local contrast image inside and outside the curve C separately. The idea is that we stick with our original assumption - the intensity of the object is statistically difference from the background. Due to the change in overall intensity across an area, the global term will fail to capture the object because of this intensity variation. However, the local contrast between object and the background remain unchanged. Therefore, by including the local term in the energy function, the local contrast information is combined with the image global statistics, and the object can then be correctly extracted from its background.

C. Level Set Formulations

In the formulation, the level set function is represented by a Lipschitz function $\phi : \Omega \rightarrow \mathbf{R}$, and the curve C is represented by the zero level set of ϕ. We define the object area ω as the positive regions of ϕ and the background area $\Omega\setminus\omega$ as the negative regions of ϕ. The overall energy function is defined,

$$J(\phi) = \alpha\, F_G(\phi) + \beta\, F_L(\phi) \tag{5}$$

We apply the same Heaviside function H and the Dirac Delta function δ_o as in [8] to divide the level set function into inside curve, outside curve or at curve C. The overall energy function can then be rewritten as,

$$\begin{aligned} J(\phi) &= \alpha \Big[\mu \int_{\Omega} \delta_o(\phi(x,y)) |\nabla\phi(x,y)| dxdy + \\ &\quad \lambda_1 \int_{\Omega} |u_o(x,y) - c_1|^2 H(\phi(x,y)) dxdy + \\ &\quad \lambda_2 \int_{\Omega} |u_o(x,y) - c_2|^2 (1 - H(\phi(x,y))) dxdy \Big] + \\ &\quad \beta \Big[\lambda_3 \int_{\Phi} |u_N(x,y) - m_1|^2 H(\phi(x,y)) dxdy + \\ &\quad \lambda_4 \int_{\Phi} |u_N(x,y) - m_2|^2 (1 - H(\phi(x,y))) dxdy \Big] \end{aligned} \tag{6}$$

The averaging constant c_1, c_2, m_1 and m_2 can also be rewritten in terms of the Heaviside function H accordingly as in (7).

$$
\begin{aligned}
c_1(\phi) &= \frac{\int_\Omega u_o(x,y)H(\phi(x,y))dxdy}{\int_\Omega H(\phi(x,y))dxdy}, \\
c_2(\phi) &= \frac{\int_\Omega u_o(x,y)(1-H(\phi(x,y)))dxdy}{\int_\Omega (1-H(\phi(x,y)))dxdy}, \\
m_1(\phi) &= \frac{\int_\Phi u_N(x,y)H(\phi(x,y))dxdy}{\int_\Phi H(\phi(x,y))dxdy}, \\
m_2(\phi) &= \frac{\int_\Phi u_N(x,y)(1-H(\phi(x,y)))dxdy}{\int_\Phi (1-H(\phi(x,y)))dxdy}
\end{aligned} \tag{7}
$$

By keeping c_1, c_2, m_1 and m_2 fixed, and minimizing the overall energy function $J(\phi)$, the evolution equation can be expressed as,

$$
\begin{aligned}
\frac{\partial \phi}{\partial t} &= \delta_o(\phi)\left\{\alpha\left[\mu\, div\left(\frac{\nabla\phi}{|\nabla\phi|}\right) - \right.\right. \\
&\quad \lambda_1(u_o-c_1)^2+\lambda_2(u_o-c_2)^2\big] + \\
&\quad \left.\beta\left[-\lambda_3(u_N-m_1)^2+\lambda_4(u_N-m_2)^2\right]\right\}
\end{aligned} \tag{8}
$$

$\phi(0,x,y)=\phi_o(x,y)$ in $\mathbf{R}^2$ where ϕ_o is the initial level set function.

III. NUMERICAL APPROXIMATION

To approximate and regularize the Heaviside function H for numerical implementation, a couple of formulations were proposed in [8][10]. For ease of comparison, we follow the approximation in [8]. We then use a finite differences implicit scheme to discretize the equation of level set function.

$$
\begin{aligned}
&\Delta_-^x\phi_{i,j}=\phi_{i,j}-\phi_{i-1,j},\ \Delta_+^x\phi_{i,j}=\phi_{i+1,j}-\phi_{i,j}, \\
&\Delta_-^y\phi_{i,j}=\phi_{i,j}-\phi_{i,j-1},\ \Delta_+^y\phi_{i,j}=\phi_{i,j+1}-\phi_{i,j}
\end{aligned} \tag{9}
$$

The optimization algorithm is basically adopted from [11] for the discretization of the divergence operator and the iterative algorithm from [12]. In each iteration, ϕ_n is known. We calculate c_1, c_2, m_1 and m_2 using (7), and ϕ_{n+1} can be estimated by the following discretization and linearization of (8).

$$
\begin{aligned}
\frac{\phi_{i,j}^{n+1}-\phi_{i,j}^n}{\Delta t} &= \alpha\,\delta_h(\phi_{i,j}^n)\times \\
&\left[\frac{u}{h^2}\Delta_-^x\left(\frac{\Delta_+^x\phi_{i,j}^{n+1}}{\sqrt{(\Delta_+^x\phi_{i,j}^n)^2/h^2+(\phi_{i,j+1}^n-\phi_{i,j-1}^n)^2/2h^2}}\right)+\right. \\
&\frac{\mu}{h^2}\Delta_-^y\left(\frac{\Delta_+^y\phi_{i,j}^{n+1}}{\sqrt{(\Delta_+^y\phi_{i,j}^n)^2/h^2+(\phi_{i+1,j}^n-\phi_{i-1,j}^n)^2/2h^2}}\right)- \\
&\lambda_1(u_{o,i,j}-c_1(\phi^n))^2+\lambda_2(u_{o,i,j}-c_2(\phi^n))^2\big]+ \\
&\beta\left[-\lambda_3(u_{N,i,j}-m_1(\phi^n))^2+\lambda_4(u_{N,i,j}-m_2(\phi^n))^2\right]
\end{aligned} \tag{10}
$$

where h is the space step, Δt is the time step.

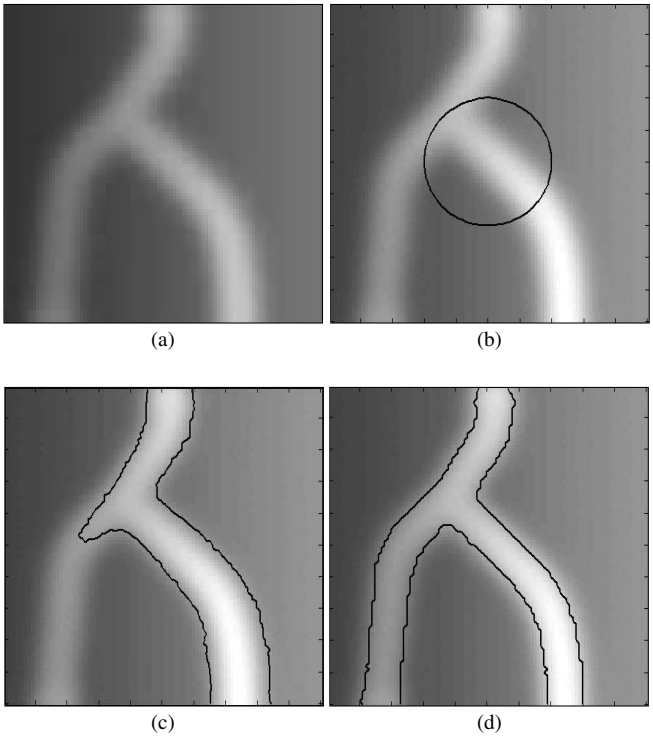

Fig. 1. Simulated images with imbalance light intensity. (a) Original image. (b) Initial contour. (c) Result of the Chan-Vese model. (d) Results of the proposed model which adapts to the changes of light intensity and extracts the entire vessel correctly.

IV. EXPERIMENTAL RESULTS

In this section, we show a number of examples to demonstrate the capability of the proposed model. We will start with a simulated image to illustrate the idea behind and then followed by a couple of real clinical angiograms for feasibility tests. In our experiments, the regulating parameters α, β, μ, λ_1, λ_2, λ_3, and λ_4 are all set to 1.0. This assumes that all the terms are treated equally important in the evolutions.

Fig. 1(a) shows a simulated image suffers from intensity variations. We simulate this phenomenon since it happen in most of the practical medical images. The initial contour is shown in Fig. 1(b). Fig. 1(c) shows the result of the Chan-Vese model [8] which cannot cop with the change of image contrast and fails to extract the whole vessel. This is because the model measures the global statistics without taking the local contrast into account. In contrast, our model measures the local image contrast by the local contrast function which is combined with the global term as the energy function for curve evolution. In Fig. 1(d), our model extracts the entire vessel correctly.

Two clinical angiograms are shown in Fig. 2 and 3 for feasibility test. The 127x104-pixel angiogram shown in Fig. 2 is obtained from [13] where the Chan-Vese model was applied and confirmed to be failed to extract the entire vessel. The original angiogram shows a couple of common artifacts in medical images. The vessel is blurry without sharp edges which causes edge based active contour to fail, and there is

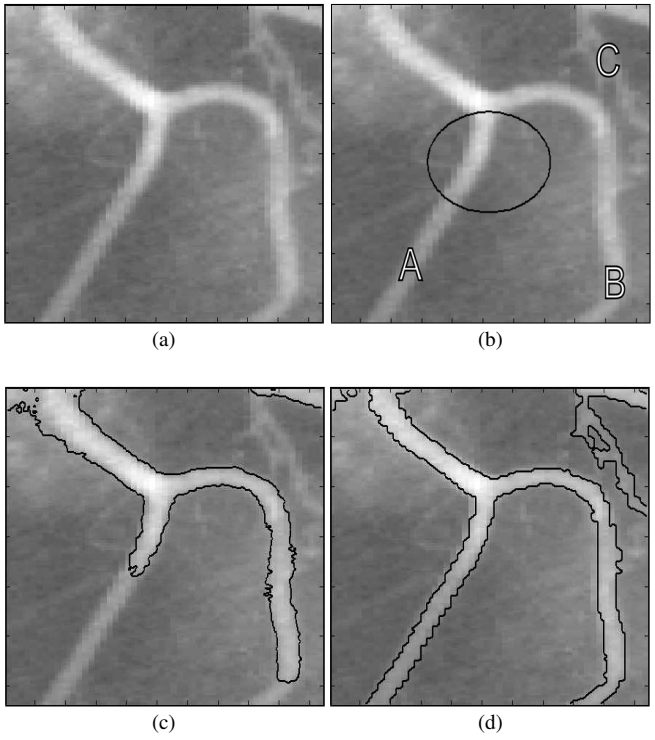

Fig. 2. Clinical angiogram. (a) Original image. (b) Initial contour. (c) Result of the Chan-Vese model. (d) Result of the proposed model which is able to extract the vessel structure correctly at A, B, and C.

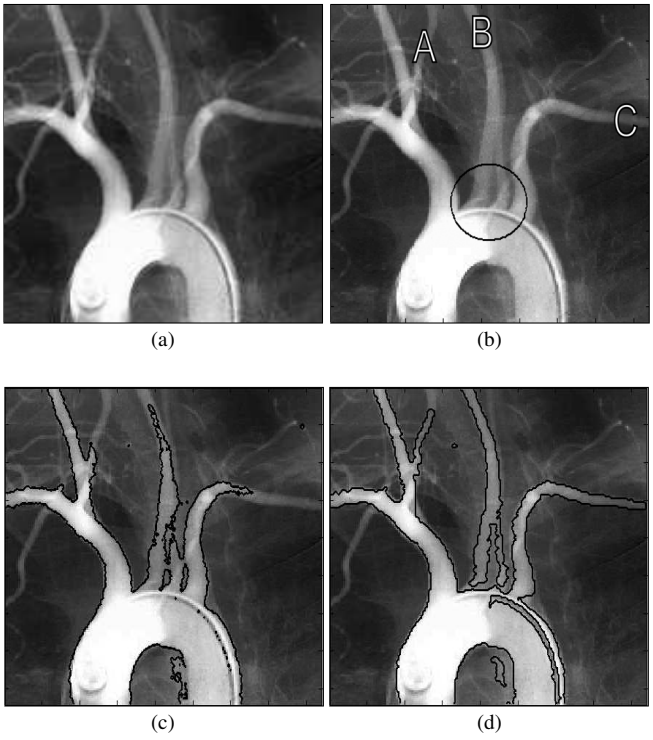

Fig. 3. The angiogram of the aortic arch. (a) Original image. (b) Initial contour. (c) Result of the Chan-Vese model. (d) Result of the proposed model which provides clear and extended vessels at A, B, and C.

uneven intensity distribution across the image. In Fig. 2(b), the same initial contours are set at the centre of the image for both Chan-Vese model and our proposed model. Fig. 2(c) shows the result of Chan-Vese model which cannot cop with the change of intensity distribution. Since the intensity values of the vessel differ greatly at different parts of the vessel, Chan-Vese model gets stuck due to the global statistical constraint and cannot capture the vessel completely. In Fig. 2(d), our proposed model extracts the entire vessel structure correctly as shown at location A, B, and C. Especially, locations A and B are the major vessels in the image.

Another example is shown in Fig. 3. It is a 168x168-pixel angiogram of the aortic arch. The Chan-Vese model can only extract parts of the right vertebral artery at A, the left carotid artery at B, and the left subclavian artery at C. It is shown that the left subclavian artery suffers from serious intensity changes along its path. Our proposed model makes use of the local term to adaptively extract the entire vessels successfully.

V. CONCLUSIONS

We have introduced a novel active contour model for vessel extraction. This model is defined based on the level set method with an energy function which is optimized according to both local and global image properties. The model is not only applicable to object with blurry boundaries, but also adaptive to the local contrast for better vessel extraction. In future research, this model can also be applied to other medical images where there are often ill-defined objects with uncertain boundaries.

REFERENCES

[1] M. Kass, A. Witkin, and D. Terzopoulos, "Snakes: Active Contour Modes", *International Journal of Computer Vision*, 321-331, 1988.
[2] C. Xu and J.L. Prince, "Snakes, Shapes, and Gradient Vector Flow", *IEEE Trans. Image Processing*, vol. 7, no. 3, Mar. 1998.
[3] K.W. Sum and P.Y.S. Cheung, "A Fast Parametric Snake Model with Enhanced Concave Object Extraction Capability", *Proceedings of IEEE ISSPIT*, 2006.
[4] S. Osher and J.A. Sethian, "Fronts Propagating with Curvature-dependent Speed: Algorithms Based on Hamilton-Jacobi Formulation", *Journal Computational Physics*, vol. 79, pp. 12-49, 1988.
[5] R. Malladi, J.A. Sethian, and B.C. Vemuri, "Shape Modeling with Front Propagation: A Level Set Approach", *IEEE Trans. PAMI*, vol. 17, no. 2, Feb 1995.
[6] V. Caselles, F. Catte, T. Coll, and F. Dibos, "A geometric model for active contours in image processing", *Numer. Math.*, vol. 66, pp. 1-31, 1993.
[7] V. Caselles, R. Kimmel, and G. Sapiro, "On Geodesic Active Contours", *International Journal of Computer Vision*, vol. 22, no. 1, pp. 61-79, 1997.
[8] T.F. Chan and L.A. Vese, "Active Contours Without Edges", *IEEE Trans. Image Processing*, vol. 10, no. 2, pp. 266-277, 2001.
[9] C. Kirbas and F. Quek, "A Review of Vessel Extraction Techniques and Algorithms", *ACM Computing Surveys*, vol. 36, no. 2, pp.81-121, June 2004.
[10] H.K. Zhao, T. Chan, B. Merriman, and S. Osher, "A Variational Level Set Approach to Multiphase Motion", *Journal Computational Physics*, vol. 127, pp. 179-195, 1996.
[11] L. Rudin, S. Osher, and E. Fatemi, "Nonlinear Total Variation Based Noise Removal Algorithms", *Phys. D.*, vol. 60, pp. 259-268, 1992.
[12] G. Arbert and L. Vese, "A Variational Method in Image Recovery", *SIAM Journal Numer. Analy.*, vol. 34, no. 5, pp. 1948-1979, 1997.
[13] *http://www.engr.uconn.edu/∼cmli/research/*